5598 *Inorg. Chem.* **2010**, *49*, 5598–5602
DOI: 10.1021/ic100495b

Inorganic Chemistry
Article

Synthesis of Alkali Metal Indium Thiophosphates Containing the Discrete Anions $[In(PS_4)(PS_5)_2]^{6-}$ and $[In(PS_4)_2(PS_5)]^{6-}$

Alexander Rothenberger, Collin Morris, and Mercouri G. Kanatzidis*

Department of Chemistry, Northwestern University, 2145 Sheridan Road, Evanston, Illinois 60208

Received March 15, 2010

The first discrete anionic indium thiophosphate complexes are reported. The structures of $K_6[In(PS_4)_{1.5}(PS_5)_{1.5}]$ (**1**), $Rb_6[In(PS_4)(PS_5)_2]$ (**2**), and $Cs_6[In(PS_4)_{1.5}(PS_5)_{1.5}]$ (**3**) all contain an anionic moiety consisting of octahedrally coordinated indium surrounded by the thiophosphate anions $[PS_4]^{3-}$ and the new $[PS_5]^{3-}$ ion. The conformation and bonding of the unsymmetric chelate ligand $[PS_5]^{3-}$ to indium give rise to different anions of the general formula $[In(PS_4)_{1+x}(PS_5)_{2-x}]^{6-}$ ($x = 0, 0.5$). The anionic moiety in $K_6[In(PS_4)_{1.5}(PS_5)_{1.5}]$ (**1**) consists of cocrystallizing λ-$[In(PS_4)_2(PS_5)]^{6-}$ and $\Lambda\lambda\delta$-$[In(PS_4)(PS_5)_2]^{6-}$ anions in a ratio of 1:1 (and their enantiomers). In $Rb_6[In(PS_4)(PS_5)_2]$ (**2**), no cocrystallizatzion of anions was observed, and only the $\Lambda\lambda\lambda$-$[In(PS_4)(PS_5)_2]^{6-}$ anion (and its enantiomer) is present. $Cs_6[In(PS_4)_{1.5}(PS_5)_{1.5}]$ (**3**) shows the same disorder between $[PS_4]^{3-}$ and $[PS_5]^{3-}$ ions as in **1**. In **3**, however, the octahedrally coordinated indium atom and thiophosphate ligands form a $\Lambda\delta\delta$-$[In(PS_4)(PS_5)_2]^{6-}$ anion cocrystallizing with δ-$[In(PS_4)_2(PS_5)]^{6-}$. Additionally, ordered $Rb_6[In(PS_4)(PS_5)_2]$ (**2**) was characterized by ^{31}P magic angle spinning NMR, Raman spectroscopy, UV−vis solid-state absorption spectroscopy, thermogravimetric analysis, differential thermal analysis, and energy dispersive X-ray analysis.

Introduction

Polychalcophosphate fluxes are widely applicable for the discovery of new ternary and quaternary solid-state thiophosphate and selenophosphate compounds.[1] The formation of these fluxes takes place by in situ fusion of A_2Q, P_2Q_5 and Q (Q = S, Se) and yields $[P_yQ_z]^{n-}$ ligands (A = alkali metal, Q = S, Se) that, in the presence of metal ions, coordinate and build new materials with potential application, e.g., in nonlinear optics,[2,3] as phase-change materials,[2,4,5] etc. The variation of the flux composition or direct combination reactions in different A:Q ratios can stabilize different ligands, such as the thiophosphate anions $[PS_4]^{3-}$,[6−8] $[P_2S_6]^{4-}$,[9] $[P_2S_7]^{4-}$,[10,11] $[P_2S_{10}]^{4-}$,[12] and $[P_3S_{10}]^{5-}$.[13] In order to access molecular compounds, it was demonstrated by the synthesis of the thiophosphate salts $K_6[Cr_2(PS_4)_4]$ and $Na_6[Pb_3(PS_4)_4]$ and the selenophosphate salts $A_5[Sn(PSe_5)_3]$ (A = K, Rb) and $A_6[Sn_2Se_4(PSe_5)_2]$ (A = Rb, Cs) that a direct combination or high-basicity flux reaction with increased concentration of $[P_yQ_z]^{n-}$ ligands can be used.[14−16] Recently, we have described surprising structural diversity in the $K_2Q/P_2Q_5/Q/In$ (Q = S, Se) system.[17] During efforts to extend this investigation to mixed thio-tellurophosphates, however, we obtained new compounds containing discrete anionic thiophosphate complexes of indium. These contain $[PS_4]^{3-}$ and the new $[PS_5]^{3-}$ chalcophosphate ligand. In the presence of alkali metal ions, the different arrangement of chalcophosphate ions around octahedrally coordinated In^{3+} gives rise to a new series of discrete anionic indium thiophosphate complexes.

*Corresponding author. Fax: +1-847-491-5937. E-mail: m-kanatzidis@northwestern.edu.

(1) Kanatzidis, M. G. *Curr. Opin. Solid State Mater. Sci.* **1997**, *2*, 139.
(2) Chung, I.; Malliakas, C. D.; Jang, J. I.; Canlas, C. G.; Weliky, D. P.; Kanatzidis, M. G. *J. Am. Chem. Soc.* **2007**, *129*, 14996.
(3) Banerjee, S.; Malliakas, C. D.; Jang, J. I.; Ketterson, J. B.; Kanatzidis, M. G. *J. Am. Chem. Soc.* **2008**, *130*, 12270.
(4) Chung, I.; Do, J.; Canlas, C. G.; Weliky, D. P.; Kanatzidis, M. G. *Inorg. Chem.* **2004**, *43*, 2762.
(5) Chung, I.; Jang, J. I.; Gave, M. A.; Weliky, D. P.; Kanatzidis, M. G. *Chem. Commun.* **2007**, 4998.
(6) Elder, S. H.; Vanderlee, A.; Brec, R.; Canadell, E. *J. Solid State Chem.* **1995**, *116*, 107.
(7) Wu, Y. D.; Bensch, W. *Inorg. Chem.* **2008**, *47*, 7523.
(8) Milot, S.; Wu, Y.; Näther, C.; Bensch, W.; Klepp, K. O. *Z. Anorg. Allg. Chem.* **2008**, *634*, 1575.
(9) Klingen, W.; Eulenberger, G.; Hahn, H. *Z. Anorg. Allg. Chem.* **1973**, *401*, 97.
(10) McCarthy, T. J.; Kanatzidis, M. G. *Chem. Mater.* **1993**, *5*, 1061.
(11) Durand, E.; Evain, M.; Brec, R. *J. Solid State Chem.* **1993**, *102*, 146.
(12) Aitken, J. A.; Canlas, C.; Weliky, D. P.; Kanatzidis, M. G. *Inorg. Chem.* **2001**, *40*, 6496.
(13) Hess, R. F.; Abney, K. D.; Burris, J. L.; Hochheimer, H. D.; Dorhout, P. K. *Inorg. Chem.* **2001**, *40*, 2851.
(14) Derstroff, V.; Ksenofontov, V.; Gütlich, P.; Tremel, W. *Chem. Commun.* **1998**, 187.
(15) Chondroudis, K.; Kanatzidis, M. G. *Chem. Commun.* **1996**, 1371.
(16) Aitken, J. A.; Kanatzidis, M. G. *Inorg. Chem.* **2001**, *40*, 2938.
(17) Rothenberger, A.; Wang, H. H.; Chung, D.; Kanatzidis, M. G. *Inorg. Chem.* **2010**, *49*, 1144.

Published on Web 05/05/2010
© 2010 American Chemical Society

Experimental Section

Starting materials were obtained from commercial sources. Sulfur was purified by melting under dynamic vacuum in order to remove volatile impurities.[18] Alkali metal sulfides were prepared in liquid ammonia.[19] Originally, $K_6[In(PS_4)_{1.5}(PS_5)_{1.5}]$ (**1**) was obtained from a reaction of K_2S, S, P_2S_5, and InTe at 350 °C. The direct combination reaction was subsequently used for the preparation of $K_6[In(PS_4)_{1.5}(PS_5)_{1.5}]$ (**1**): A mixture of 68 mg (0.61 mmol) of K_2S, 96 mg (1.23 mmol) of P_2S_5, 20 mg (0.61 mmol) of S, and 140 mg (1.22 mmol) of In was sealed in a fused silica tube under vacuum. The reaction was heated to 500 °C over the course of 6 h and kept at this temperature for 3 days. Cooling to 100 °C (5 K/h) gave a red-orange solid that contained crystals of **1** (yield 95%). $Rb_6[In(PS_4)(PS_5)_2]$ (**2**) (Rb_2S, 124 mg, 0.61 mmol) and $Cs_6[In(PS_4)_{1.5}(PS_5)_{1.5}]$ (**3**) (Cs_2S, 182 mg, 0.61 mmol) were synthesized in the same way (yield 95% for **2**, ca. 30% for **3**). Very few dark-red particles were formed together with yellow crystals of **2**. By energy dispersive X-ray analysis (EDS), the composition of these particles is identical to **2**. $Cs_4[P_2S_{10}]$ was identified as a crystalline byproduct during the formation of **3**. The presence of metals, P and S, was confirmed by semiquantitative EDS on a Hitachi S-3400 scanning electron microscope (SEM) equipped with a PGT energy dispersive X-ray analyzer. Found: **1**: P 13.5, S 58.9, K 23.0, In 4.5; $InK_6P_3S_{13.50}$ requires P 12.7, S 57.4, K 25.5, In 4.3 at. %; **2**: P 13.1, S 60.4, Rb 22.5, In 4.0; $InP_3Rb_6S_{14}$ requires P 12.5, S 58.3, Rb 25.0, In 4.1 at. %; **3**: P 14.3, S 62.9, In 4.0, Cs 18.4; $Cs_6InP_3S_{13.50}$ requires P 12.7, S 57.4, In 4.3, Cs 25.6 at. %. Powder X-ray diffraction (PXRD) analyses were performed using an INEL CPS120 powder diffractometer (flat geometry) with graphite monochromatized Cu-K_α radiation. The thermogravimetric analysis (TGA) measurements were performed on a Shimadzu TGA-50 thermogravimetric analyzer in aluminum boats under a N_2 flow. Differential thermal analyses (DTA) were performed on a Shimadzu DTA-50 thermal analyzer in sealed quartz ampules. To assess congruent melting, we compared the PXRD patterns before and after DTA experiments. The stability and reproducibility of the samples were monitored by running multiple heating/cooling cycles.

Solid-state absorption spectra of **2** (S2) were measured on a U-6000 microscopic FT spectrophotometer using single crystals suspended in paraffin oil. Optical diffuse reflectance measurements were performed at room temperature using a Shimadzu UV-3101PC double beam, double monochromator spectrophotometer. ^{31}P magic angle spinning (MAS) NMR spectra were recorded on a Varian Mercury 400 spectrometer and referenced to $NH_4H_2PO_4$ (δ 0.8). The delay time between scans was 60 s. The Raman measurement was carried out at room temperature on a DeltaNu Advantage NIR spectrometer equipped with a CCD camera detector using 785 nm radiation from a diode laser. A maximum power of 60 mW and a beam diameter of 35 μm were used. The spectrum was collected using an integration time of 3 s. The Raman spectrum was calibrated against an American Society for Testing and Materials (ASTM) polystyrene standard.

X-ray Crystallographic Studies. Data for **1**−**3** were collected on STOE IPDS 2T and STOE IPDS 2 diffractometers using graphite-monochromated Mo-K_α radiation (λ = 0.71073 Å). The structures were solved by direct methods and refined by full-matrix least-squares on F^2 (all data) using the SHELXTL program package.[20] Numerical absorption corrections were performed for **1**−**3**. A summary of crystal data and refinement parameters is given in Table 1. Crystal coordinates are listed in Table 2.

Table 1. Details of the X-ray Data Collection and Refinements for $K_6[In(PS_4)_{1.5}(PS_5)_{1.5}]$ (**1**), $Rb_6[In(PS_4)(PS_5)_2]$ (**2**), and $Cs_6[In(PS_4)_{1.5}(PS_5)_{1.5}]$ (**3**)

compound	**1**	**2**	**3**
formula	$InK_6P_3S_{13.50}$	$InP_3Rb_6S_{14}$	$Cs_6InP_3S_{13.50}$
formula weight	875.14	1169.39	1438.00
T/K	200(2)	293(2)	293(2)
crystal system	triclinic	monoclinic	triclinic
space group	P-1	$C2/c$	P-1
a/Å	10.8546(7)	19.695(2)	8.5474(5)
b/Å	11.0628(7)	10.9763(8)	10.8068(6)
c/Å	12.8098(9)	13.054(1)	16.6108(9)
α/°	65.878(5)	90.00	78.192(5)
β/°	86.249(6)	107.539(6)	77.332(5)
γ/°	64.173(5)	90.00	81.150(5)
Z	2	4	2
V/Å^3	1251.8(1)	2690.8(4)	1455.7(1)
ρ/g·cm^{-3}	2.322	2.887	3.281
μ/mm^{-1}	3.250	12.919	9.332
F(000)	848	2160	1280
reflections collected	19 947	12 440	13 817
unique data	6650	3627	7216
R_{int}	0.0720	0.1046	0.0518
parameters	244	110	262
$R_1{}^a$ [$I > 2\sigma(I)$]	0.0717	0.0595	0.0486
$wR_2{}^b$ (all data)	0.0965	0.1306	0.1234

$^a R_1 = \sum||F_0| - |F_c||/\sum|F_0|$. $^b wR_2 = \sum w(F_0^2 - F_c^2)^2/\sum w(F_0^2)^2\}^{1/2}$.

Results and Discussion

The direct combination reaction of A_2S, S, P_2S_5, and indium (A = K, Rb, Cs) in the appropriate ratio necessary for the preparation of alkali metal derivatives of the previously obtained $K_6[In(PS_4)_{1.5}(PS_5)_{1.5}]$ gave, after cooling to room temperature, solidified melts from which crystals of $K_6[In(PS_4)_{1.5}(PS_5)_{1.5}]$ (**1**), $Rb_6[In(PS_4)(PS_5)_2]$ (**2**), and $Cs_6[In(PS_4)_{1.5}(PS_5)_{1.5}]$ (**3**) were isolated (Scheme 1).

In the melt that contains $K_6[In(PS_4)_{1.5}(PS_5)_{1.5}]$ (**1**), not all the isolated solid was single-crystalline but showed identical composition by EDS. The orange crystals of $Rb_6[In(PS_4)(PS_5)_2]$ (**2**) were isolated with only a small amount of dark-red crystals present. By EDS analysis, these have the same composition as **2**. In the case of Cs, crystals of $Cs_6[In(PS_4)_{1.5}(PS_5)_{1.5}]$ (**3**) and $Cs_4P_2S_{10}$ were obtained.[12] The bandgaps of **1**−**3** are 1.9−2.1 eV. The crystal structure analysis of **1**−**3** revealed a central $[In(PS_4)_{1+x}(PS_5)_{2-x}]^{6-}$ (x = 0, 0.5) anionic moiety is formed in all reactions (Figure 1).

$K_6[In(PS_4)_{1.5}(PS_5)_{1.5}]$ (**1**) crystallizes in the triclinic space group P-1. The anionic moiety in **1** consists of cocrystallizing anions λ-$[In(PS_4)_2(PS_5)]^{6-}$ and $\Lambda\lambda\delta$-$[In(PS_4)(PS_5)_2]^{6-}$ anions in a ratio of 1:1 (and their enantiomers). The indium atom in **1** exhibits a distorted octahedral coordination environment. Observed K−S (ca. 3.3 Å) and S−In (*ca.* 2.5 Å) bond distances are normal and in the range of what has been reported previously (2.4−2.6 Å In−S, 3.1−3.6 Å K···S).[21] In order to confirm the presence of the different anions

(18) Susman, S.; Rowland, S. C.; Volin, K. J. *J. Mater. Res.* **1992**, *7*, 1526.
(19) (a) Klemm, W.; Sodomann, H.; Langmesser, P. *Z. Anorg. Allg. Chem.* **1939**, *241*, 281. (b) Huang, S. P.; Kanatzidis, M. G. *Inorg. Chem.* **1991**, *30*, 1455–1466. (c) Kanatzidis, M. G.; Park, Y. *Chem. Mater.* **1990**, *2*, 99–101. (d) Manos, M. J.; Iyer, R. G.; Quarez, E.; Liao, J. H.; Kanatzidis, M. G. *Angew. Chem.—Int. Ed.* **2005**, *44*, 3552–3555.
(20) Sheldrick, G. M. *SHELXTL*, v. 5.1; University of Göttingen: Göttingen, Germany**1997**.
(21) Allen, F. H.; Bellard, S.; Brice, M. D.; Cartwright, B. A.; Doubleday, A.; Higgs, H.; Hummelink, T.; Hummelinkpeters, B. G.; Kennard, O.; Motherwell, W. D. S.; Rodgers, J. R.; Watson, D. G. *Acta Crystallogr., Sect. B: Struct. Sci* **1979**, *35*, 2331.

Table 2. Atomic Coordinates and Displacement Parameters (in Å^2) for $K_6[In(PS_4)_{1.5}(PS_5)_{1.5}]$ (**1**), $Rb_6[In(PS_4)(PS_5)_2]$ (**2**), and $Cs_6[In(PS_4)_{1.5}(PS_5)_{1.5}]$ (**3**)

$K_6[In(PS_4)_{1.5}(PS_5)_{1.5}]$ (**1**)

Label	*x*	*y*	*z*	Occupancy	U_{eq}[a]
K(1)	0.79871(17)	−0.23987(15)	0.93440(12)	1	0.0275(3)
K(2)	0.31566(16)	0.03965(17)	0.84350(14)	1	0.0262(3)
K(3)	−0.2625(2)	0.3406(2)	0.9560(2)	1	0.0509(6)
K(4)	0.45010(17)	0.27186(18)	0.47009(13)	1	0.0305(3)
K(5)	−0.10397(18)	1.26911(17)	0.64784(13)	1	0.0288(3)
K(6)	−0.11928(16)	0.89007(16)	0.63770(15)	1	0.0302(4)
In(1)	0.31753(5)	0.49919(5)	0.73650(4)	1	0.01324(10)
P(1)	0.2328(11)	0.8883(7)	0.6783(10)	0.50	0.0147(13)
P(1′)	0.2563(10)	0.8448(7)	0.6848(9)	0.50	0.0144(13)
P(2)	−0.02545(16)	0.49206(17)	0.78044(13)	1	0.0130(3)
P(3)	0.59944(16)	0.17847(16)	0.79320(13)	1	0.0132(3)
S(1)	0.20942(18)	0.77940(17)	0.57802(14)	1	0.0225(3)
S(2)	0.4358(3)	0.7493(3)	0.7714(3)	0.50	0.0135(5)
S(2′)	0.4017(3)	0.6374(4)	0.8078(3)	0.50	0.0246(7)
S(3)	0.09735(19)	0.9195(2)	0.77672(18)	1	0.0303(4)
S(4)	0.2494(4)	1.0714(4)	0.5796(3)	0.50	0.0254(7)
S(4′)	0.3414(5)	0.9788(5)	0.6027(4)	0.50	0.0335(9)
S(5)	0.4317(3)	0.5494(3)	0.8724(3)	0.50	0.0156(6)
S(6)	−0.22780(16)	0.62725(17)	0.75973(14)	1	0.0189(3)
S(7)	0.00577(16)	0.54592(17)	0.60601(13)	1	0.0172(3)
S(8)	0.21557(17)	0.4228(2)	0.61658(15)	1	0.0220(3)
S(9)	0.09141(15)	0.55586(16)	0.84559(13)	1	0.0139(3)
S(10)	0.02535(17)	0.27708(17)	0.86317(15)	1	0.0204(3)
S(11)	0.55383(17)	0.38184(16)	0.65522(14)	1	0.0193(3)
S(12)	0.45172(17)	0.22958(18)	0.90079(14)	1	0.0222(3)
S(13)	0.78808(17)	0.08368(18)	0.88121(15)	1	0.0222(3)
S(14)	0.58017(17)	0.04478(17)	0.73237(14)	1	0.0195(3)

$Rb_6[In(PS_4)(PS_5)_2]$ (**2**)

Label	*x*	*y*	*z*	U_{eq}
Rb(1)	0.09448(4)	0.11846(8)	0.58730(6)	0.0375(2)
Rb(2)	0.21555(4)	0.11271(7)	0.35093(7)	0.0335(2)
Rb(3)	0.38320(4)	0.18312(7)	0.00971(6)	0.0317(2)
In(1)	0	0.36708(6)	0.25	0.0207(2)
P(1)	0.19173(9)	0.4672(2)	0.3294(1)	0.0192(3)
P(2)	0	0.0568(2)	0.25	0.0183(4)
S(1)	0.0414(1)	0.1747(2)	0.1599(1)	0.0252(4)
S(2)	0.0424(1)	0.5157(2)	0.1310(1)	0.0254(4)
S(3)	0.12936(9)	0.3734(2)	0.4036(1)	0.0220(3)
S(4)	0.2306(1)	0.3629(2)	0.2362(2)	0.0282(4)
S(5)	0.2353(1)	0.0684(2)	0.0664(2)	0.0311(4)
S(6)	0.3755(1)	0.1060(2)	0.2600(1)	0.0238(3)
S(7)	0.4246(1)	0.4530(2)	0.1508(2)	0.0332(4)

$Cs_6[In(PS_4)_{1.5}(PS_5)_{1.5}]$ (**3**)

Label	*x*	*y*	*z*	Occupancy	U_{eq}
Cs(1)	0.01399(8)	0.08770(8)	0.32885(5)	1	0.0546(2)
Cs(2)	0.05140(6)	0.36553(7)	0.77349(4)	1	0.0449(2)
Cs(3)	0.2597(2)	0.5977(2)	0.48514(9)	0.50	0.0610(4)
Cs(3′)	0.1705(2)	0.6528(2)	0.46675(8)	0.50	0.0547(4)
Cs(4)	0.25338(6)	0.99488(5)	0.05422(4)	1	0.0366(1)
Cs(5)	0.44907(8)	0.06618(5)	0.66888(4)	1	0.0420(1)
Cs(6)	0.26383(5)	0.43186(4)	0.00256(3)	1	0.0291(1)
In(1)	0.52046(6)	0.62375(5)	0.73552(3)	1	0.0231(1)
P(1)	0.7141(9)	0.7494(8)	0.5425(5)	0.50	0.025(1)
P(1′)	0.7555(8)	0.7701(8)	0.5263(5)	0.50	0.025(1)
P(2)	0.5606(2)	0.3078(2)	0.7865(1)	1	0.0186(3)
P(3)	0.1868(2)	0.7880(2)	0.8895(1)	1	0.0226(3)
S(1)	0.4673(6)	0.7650(4)	0.6000(3)	0.50	0.0320(8)
S(1′)	0.5286(4)	0.7196(4)	0.5180(2)	0.50	0.0270(7)
S(2)	0.7416(7)	0.6578(5)	0.4463(3)	0.50	0.051(1)
S(2′)	0.8904(6)	0.7161(5)	0.4236(3)	0.50	0.047(1)
S(3)	0.8127(2)	0.6458(2)	0.6365(1)	1	0.0310(4)
S(4)	0.787(1)	0.9210(7)	0.5095(4)	0.50	0.042(2)

Table 2. Continued

$Cs_6[In(PS_4)_{1.5}(PS_5)_{1.5}]$ (**3**)

Label	*x*	*y*	*z*	Occupancy	U_{eq}
S(4′)	0.742(1)	0.9537(7)	0.5278(5)	0.50	0.041(2)
S(5′)	0.3735(5)	0.7646(4)	0.6236(2)	0.50	0.0254(7)
S(6)	0.4597(2)	0.4213(2)	0.6904(1)	1	0.0273(3)
S(7)	0.6259(2)	0.4408(2)	0.8442(1)	1	0.0228(3)
S(8)	0.7577(2)	0.1981(2)	0.7390(1)	1	0.0331(4)
S(9)	0.3959(2)	0.2045(2)	0.8651(1)	1	0.0295(4)
S(10)	0.2008(2)	0.6556(2)	0.8156(1)	1	0.0324(4)
S(11)	0.4174(2)	0.7606(2)	0.9237(1)	1	0.0262(3)
S(12)	0.5818(2)	0.7887(2)	0.8128(1)	1	0.0269(3)
S(13)	0.1400(2)	0.9665(2)	0.8344(1)	1	0.0324(4)
S(14)	0.0477(2)	0.7441(2)	1.0028(1)	1	0.0339(4)

[a] U_{eq} is defined as one third of the trace of the orthogonalized $\mathbf{U}_{ij}$ tensor.

Scheme 1. Synthesis of **1**−**3** (A = K, Rb, Cs)

$$3A_2S + In + 1.5P_2S_5 + 3.5S \xrightarrow{500°C} \begin{matrix} K_6[In(PS_4)_{1.5}(PS_5)_{1.5}]\ (\mathbf{1}) \\ Rb_6[In(PS_4)(PS_5)_2]\ (\mathbf{2}) \\ Cs_6[In(PS_4)_{1.5}(PS_5)_{1.5}]\ (\mathbf{3}) \end{matrix}$$

present in **1**, the solid residue from which crystals were broken off was ground and investigated by ^{31}P MAS NMR. The four observed resonances at δ 93 ($[PS_4]^{3-}$), 86, 83, and 79 ppm, respectively, indicated that the solid reaction product contains a mixture of λ-$[In(PS_4)_2(PS_5)]^{6-}$ and $\Lambda\lambda\delta$-$[In(PS_4)(PS_5)_2]^{6-}$ anions. The resonance at δ 93 ppm is similar to the chemical shift observed for $[PS_4]^{3-}$ in $KPbPS_4$ and $K_4Ti_2P_6S_{25}$.[22,23] The remaining resonances can tentatively be assigned to $[PS_5]^{3-}$ anions in the different chemical environments of λ-$[In(PS_4)_2(PS_5)]^{6-}$ and $\Lambda\lambda\delta$-$[In(PS_4)(PS_5)_2]^{6-}$ and to stereoisomers that may have formed. The presence of other potassium salts of $[P_yS_z]^{n-}$ anions ($Cs_4P_2S_{10}$[12] containing the $[S_3P-(S)_4-PS_3]^{4-}$ anion formed together with **3**) cannot be ruled out. $Rb_6[In(PS_4)(PS_5)_2]$ (**2**) crystallizes in the monoclinic space group $C2/c$. Unlike **1**, no cocrystallizatzion of anions was observed, and only the $\Lambda\lambda\lambda$-$[In(PS_4)(PS_5)_2]^{6-}$ anion (and its enantiomer) is present in **2**. It is assumed that a change of the alkali metal ion is responsible for the preferred crystallization of the $\Lambda\lambda\lambda$-$[In(PS_4)(PS_5)_2]^{6-}$ anion in **2**, where disulfide motifs are in a *cis* arrangement in comparison to the *trans* arrangement in the $\Lambda\lambda\delta$-$[In(PS_4)(PS_5)_2]^{6-}$ anionic moiety of **1** (Figure 1). In the ^{31}P MAS NMR of **2**, two resonances are observed at δ 99 ($[PS_4]^{3-}$) and 81 ($[PS_5]^{3-}$) ppm (Figure 2).

$Cs_6[In(PS_4)_{1.5}(PS_5)_{1.5}]$ (**3**) crystallizes in the triclinic space group $P\bar{1}$ and shows the same disorder between $[PS_4]^{3-}$ and $[PS_5]^{3-}$ ions that was already observed in **1**. In **3**, the octahedrally coordinated indium atom and thiophosphate ligands, however, form a $\Lambda\delta\delta$-$[In(PS_4)(PS_5)_2]^{6-}$ anion cocrystallizing with δ-$[In(PS_4)_2(PS_5)]^{6-}$ (Figure 1). The fact that different anions were characterized in **1**−**3** is remarkable and is most likely the result of the different counter cations present. For further studies, **2** was chosen because only one compound was detected in the ^{31}P MAS NMR spectrum and no significant amount of byproducts could be detected. In the TGA of **2**, there is a notable stepwise weight loss that

(22) Rothenberger, A.; Morris, C.; Wang, H. H.; Chung, D. Y.; Kanatzidis, M. G. *Inorg. Chem.* **2009**, *48*, 9036.
(23) Derstroff, V.; Tremel, W.; Regelsky, G.; Günne, J. S. A. D.; Eckert, H. *Solid State Sci.* **2002**, *4*, 731.

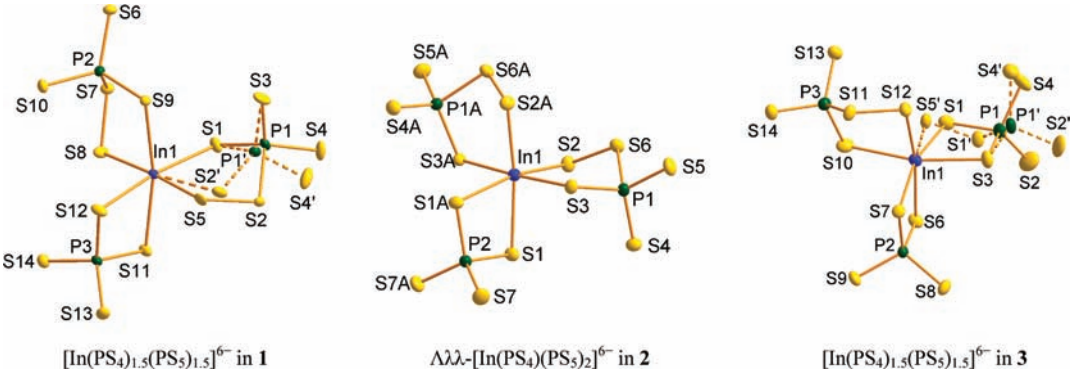

Figure 1. Structure of the anionic moiety in **1**−**3** (ellipsoids at 50% probability level). Because bond distances within the anions are similar, selected bond lengths [Å] and angles [°] are listed for **1**. In(1)−S(1) 2.6657(16), In(1)−S(2′) 2.544(3), In(1)−S(5) 2.559(3), In(1)−S(8) 2.5292(17), In(1)−S(9) 2.7012(15), In(1)−S(11) 2.6836(16), In(1)−S(12) 2.6328(17), P−S ca. 1.9−2.1, S(2)−S(5) 2.075(4), S(7)−S(8) 2.061(2), S(1)−In(1)−S(9) 91.43(5), S(1)−In(1)−S(11) 100.44(5), S(5)−In(1)−S(1) 93.61(8), S(8)−In(1)−S(1) 92.08(6), S(5)−In(1)−S(12) 79.35(8), S(8)−In(1)−S(12) 94.96(6), S(11)−In(1)−S(9) 167.67(4), S(5)−S(2)−P(1) 103.7(3), and S(8)−S(7)−P(2) 103.22(9). Corresponding distances and angles in **2** and **3** are similar to those listed. Symmetry operation for **2**: $-x, y, -z + 1/2$ (A).

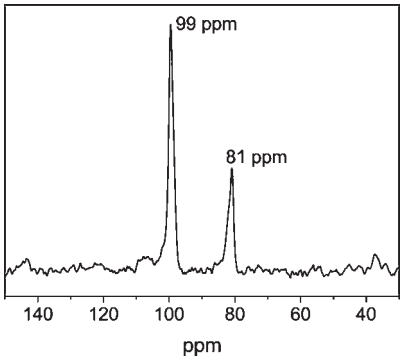

Figure 2. ^{31}P MAS NMR spectrum of **2**.

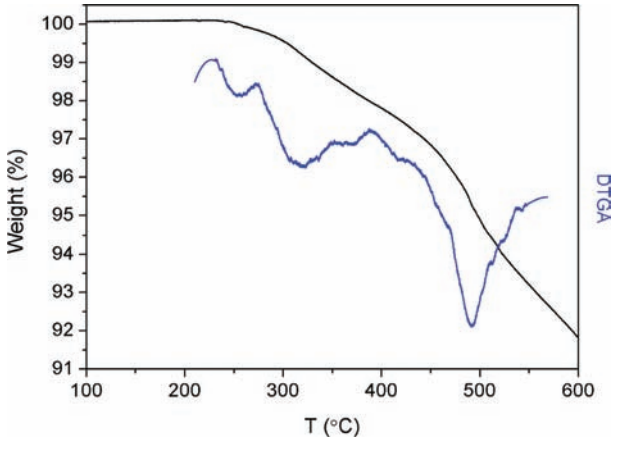

Figure 3. TGA and plotted DTGA of **2** (recorded in open Al boats under N_2 flow, 10 °C/min).

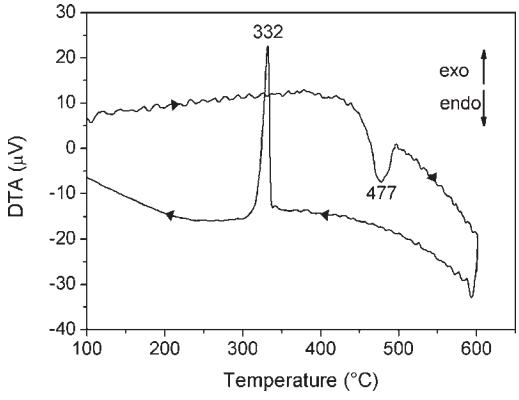

Figure 4. DTA of **2** (10 °C/min, N_2 flow, recorded in sealed quartz ampules).

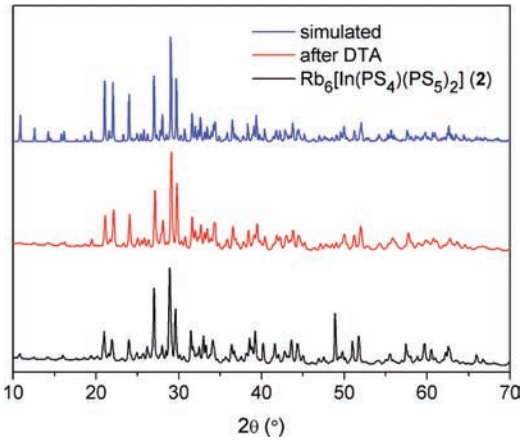

Figure 5. Experimental and simulated PXRD pattern of **2**. The crystallinity is retained after DTGA.

becomes visible in the differential thermogravimetric analysis (DTGA) plot (Figure 3).

The weight loss from ca. 220−390 °C possibly corresponds to the loss of one sulfur atom from the $[PS_5]^{3-}$ anions in $Rb_6[In(PS_4)(PS_5)_2]$ (**2**). The overall weight loss of 7% at ca. 580 °C may indicate the transformation of remaining $[PS_5]^{3-}$ into $[PS_4]^{3-}$ anions. The thermal instability of these anions may be the reason why there has been no crystallographic evidence for $[PS_5]^{3-}$ ions so far. In the DTA, this thermal decomposition is not detected. $[PS_4]^{3-}$ ions possibly reincorporate released sulfur to give $[PS_5]^{3-}$, and as such, **2** appears to be congruently melting (Figures 4 and 5 and Figure S6 in the Supporting Information).

In the Raman spectrum of **2**, the various resonances below 300 cm^{-1} point toward different P-chalcogen bending modes and In−S stretching vibrations (Figure 6).[12,24]

(24) (a) Chondroudis, K.; Hanko, J. A.; Kanatzidis, M. G. *Inorg. Chem.* **1997**, *36*, 2623. (b) Aitken, J. A.; Marking, G. A.; Evain, M.; Iordanidis, L.; Kanatzidis, M. G. *J. Solid State Chem.* **2000**, *153*, 158. (c) Hanko, J. A.; Sayettat, J.; Jobic, S.; Brec, R.; Kanatzidis, M. G. *Chem. Mater.* **1998**, *10*, 3040.

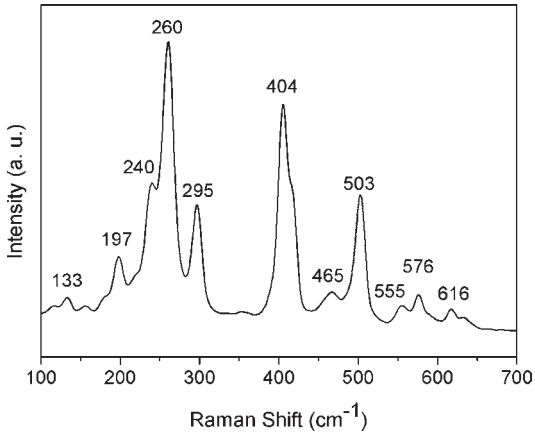

Figure 6. Raman spectrum of **2**.

The very strong peak that occurs at 404 cm^{-1} can be assigned to the symmetric stretching of the PS_4 tetrahedral unit. Vibrations at energies greater than 450 cm^{-1} are assigned to other asymmetric P-chalcogen stretching modes in the chalcophosphate units present in **2**.[25]

(25) Sourisseau, C.; Rodriguez, V.; Jobic, S.; Brec, R. *J. Raman Spectrosc.* **1999**, *30*, 1087.

Concluding Remarks

The exploration of quaternary A/M/P/Q phases is still incomplete. Our interest is particularly directed toward the development of new mixed chalcogen-containing systems. While we demonstrated structural evidence for A/In/P/S/Se phases previously, the present work initially was aimed at the A/In/P/S/Te phases. Instead, the first discrete anionic indium thiophosphate complexes were obtained. The structures of **1**−**3** all differ slightly in their anionic $[In(PS_4)_{1+x}(PS_5)_{2-x}]^{6-}$ (x = 0, 0.5) moiety. The observation of several conformations of $[PS_4]^{3-}$ and $[PS_5]^{3-}$ ions around the octahedrally coordinated indium atom gives rise to a variety of stereoisomers and may allow rare investigations of the stereochemical outcome of flux reactions. Furthermore, A/M/P/Q phases of the lighter alkali metals are currently of interest, and it is assumed that these may adopt different structures to those known for A = K, Rb, and Cs.

Acknowledgment. Financial support from the DFG (RO 3069/4-1) and from the National Science Foundation (DMR-0801855) is gratefully acknowledged.

Supporting Information Available: Powder diffraction patterns, SEM, DTA, crystallographic information files (CIF). This material is available free of charge via the Internet at http://pubs.acs.org.